*Usp. Fiz. Nauk* (Suppl.) **171** (10) 20–35 (2001) 

PACS numbers: **72.15.-v**, 72.15.Rn, 05.60.Gg, 05.45.Mt

# *Chernogolovka 2000*: Mesoscopic and strongly correlated electron systems

## 1. Localization and quantum chaos

### Order, disorder and chaos in 2D lattice of coupled Sinai billiards

M V Budantsev, Z D Kvon, A G Pogosov, J C Portal

**Abstract. Transport properties of a new kind of ballistic electron billiards — two-dimensional (2D) lattice of Sinai billiards coupled through quantum point contacts — are experimentally studied. This lattice is peculiar by simultaneous existence of the effects inherent to single Sinai billiards or quantum dots, and the features reflecting lattice properties of system. Magnetotransport measurements give very pronounced commensurability peak even if the conductivity of the lattice $G \ll e^2/h$. Consequently it preserves the properties of ballistic regular structure at these conductivity states. On the other hand, the gate voltage dependencies of G show that the system behaves as percolation one. In weak magnetic fields negative magnetoresistance (NMR) is observed. It is described by theory of chaotic weak localization developed for case of single ballistic cavity. This NMR increases in going from $G > e^2/h$ to $G \ll e^2/h$. Thus, 2D lattice of coupled Sinai billiards is a unique system where coexistence of order, disorder and chaos are clearly demonstrated.**

Quantum and classical transport in systems with dynamic chaos has been intensively studied in the past few years, since the successes of modern semiconductor technology have made it possible to obtain various experimental realizations of such systems with electron billiards as an example. At present, two varieties of these systems are studied. The first one is single billiards (regular or chaotic Bunimovich or Sinai billiards) [1–5], while the second one is macroscopic 2D (antidot lattice) [6–10] or one-dimensional [11] Sinai billiards.

This paper is the first report on the results of experimental investigation of a new system with dynamic chaos. The system was built on the basis of a 2D lattice of the large and dense antidots fabricated from a high mobility 2D electron gas in GaAs/AlGaAs heterojunction with a metallic gate evaporated on the top, that permitted us to control the conductivity of the structure in a sufficiently wide range, from $g = 0.01$ to $g = 2$.

**M V Budantsev, Z D Kvon, A G Pogosov**
Institute of Semiconductor Physics, Siberian Division of RAS, 630090 Novosibirsk, Russian Federation
**J C Portal** GHML, MPI-FKF/CNRS, BP 166, F-38042 Grenoble Cedex 9, France, INSA 135 avenue de Rangueil, 31 077 Toulouse Cedex 4, France

The square and hexagonal lattices of antidots were fabricated on the basis of a 2D electron gas with the electron density $N_S = (2-3) \times 10^{11}$ cm$^{-2}$ and the mobility $\mu = (3-8) \times 10^5$ cm$^2$ V$^{-1}$ s$^{-1}$, corresponding to the mean free path $l = (3-6)$ μm, by means of electron lithography and subsequent plasma etching. Then the NiAu or TiAu gate was evaporated on the top of the device. The samples used in the experiments were two Hall bridges with 100 μm in length and 50 μm in width. The lattice of antidots covered entirely the one Hall bridge. We investigated the samples with the lattice periods $d = 0.6$ μm and $d = 0.7$ μm. The lithographic size of antidots 0.2 μm was the same for all samples. However, owing to the depletion regions, the actual size of antidots ($a$) was larger, being approximately equal to the lattice period even before the gate evaporation.

Figure 1a shows the set of temperature dependences of the conductivity $g(T)$ for the sample AG219 with the period $d = 0.6$ μm ($\mu = 7 \times 10^5$ cm$^2$ V$^{-1}$ s$^{-1}$ at $N_S = 2 \times 10^{11}$ cm$^{-2}$ in the unpatterned part of the sample) for different values of the gate voltage. It is seen that for $g > 1$ the conductivity is practically temperature independent. More exactly, a weak logarithmic decrease of $g$ is observed, which is typical of weak localization effects. The temperature dependence becomes more noticeable for lower values of the conductivity, but it still remains weak even for $g \ll 1$. It is well described by a power law $g(T) \propto T^\alpha$, with $\alpha < 1$ for all the samples studied. Specifically, for the dependences depicted in Fig. 1a $\alpha = 0.1-0.27$ at $g \ll 1$. A similar behavior is observed for the sample with a lower mobility (AG35, $\mu = 5 \times 10^5$ cm$^2$ V$^{-1}$ s$^{-1}$) but with larger values of $\alpha = 0.3-0.66$ (Fig. 1b). The behavior of $g(T)$ described above is significantly different from the behavior of the unpatterned 2D electron gas both in silicon MOS-transistors [12] and in AlGaAs/GaAs heterojunction [13], as well as for antidot lattices with short period [14, 15]. At $g \sim 1$ a transition from the weak logarithmic dependence (weak localization regime) to the strong exponential one (strong localization regime) is observed in all these cases. In our case a weak logarithmic decrease of $g$ (for $g > 1$) is followed by a weak power law, that has not been observed in other 2D systems. Figure 2 shows the typical experimental dependence of the conductivity vs. gate voltage and the theoretical curve calculated in according to the expression depicted in the left upper part of the figure. This expression is similar to one well known in the percolation theory as the problem of sites on square lattice [16]. The theory gives the value $t = 1-1.5$ for critical index $t$, which is close to experimental one as is seen from the figure. It suggests that our system demonstrates the percolation behavior and the saddle points between antidots are the sites of square lattice.

Consider the influence of magnetic field. It is well known that in AlGaAs/GaAs heterojunctions, a transition from an

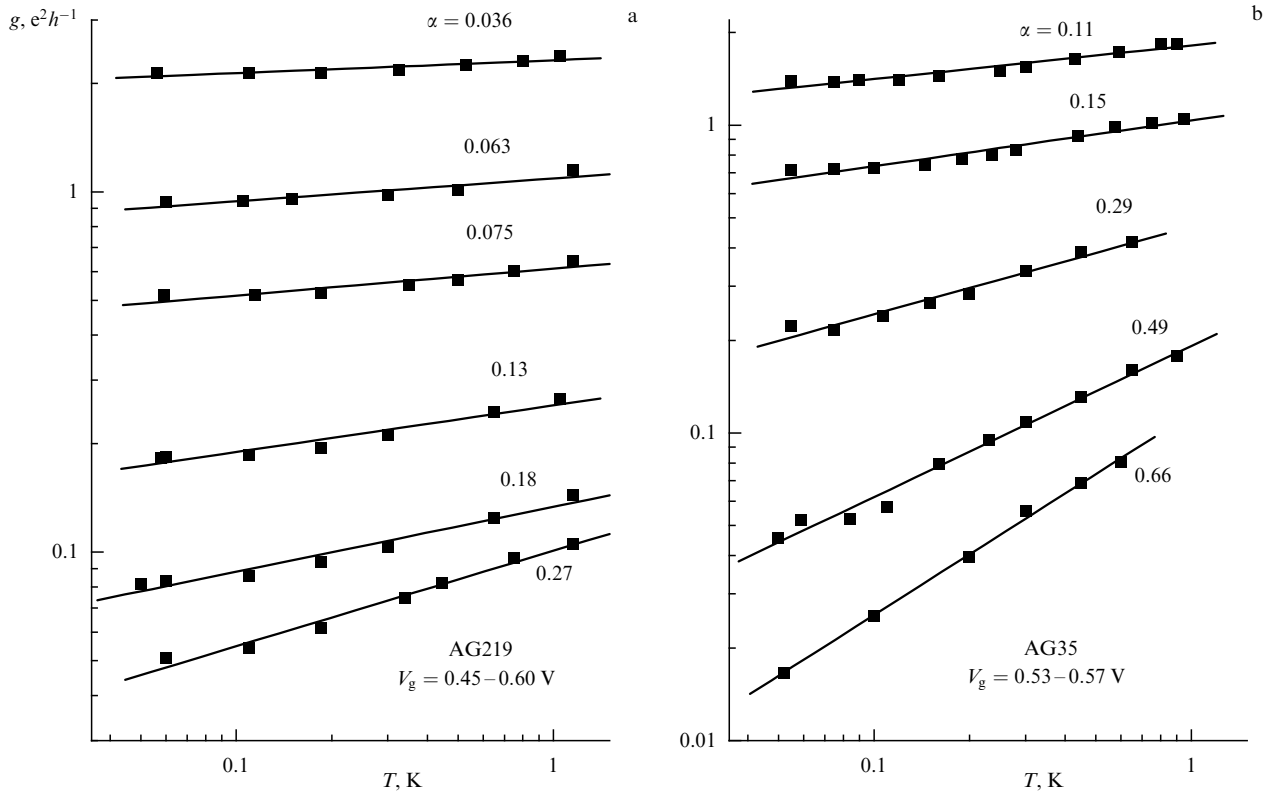


**Figure 1.** Temperature dependences of the conductivity at the transition from $g > 1$ to $g \ll 1$. Solid lines are $g \propto T^{\alpha}$.

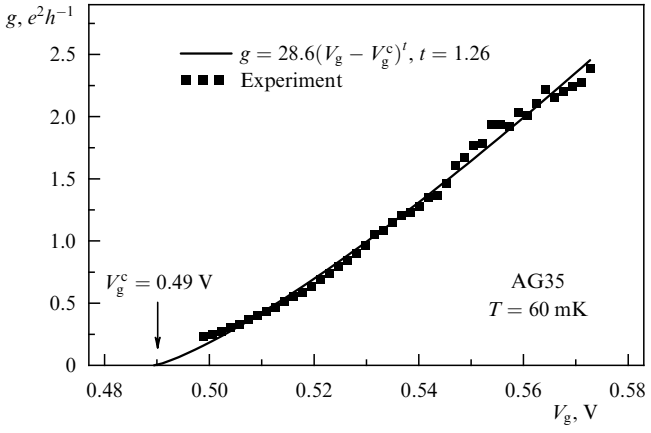


**Figure 2.** Experimental and calculated gate voltage dependences of the conductivity for the square lattice.

insulator to the quantum-Hall liquid is observed at $g < 1$ and an applied magnetic field. The transition is characterized by the critical point $B_c$ and $g_c \approx 0.5-1$ [13]. Our samples exhibit a radically different picture. It is seen from Fig. 3 that for all values of $g(B = 0)$ at the magnetic fields $B \approx 1$ T the transition takes place from weak power-law dependence $g(T)$ to no temperature dependence at all. Moreover, the transition is of different kind, for there is no critical point, and the metallic behavior extends for $g \ll 1$. Figure 3 also shows an interesting behavior in weak magnetic field. For all values of $g$, the negative magnetoresistance is observed at the magnetic fields $B < 0.05$ T, followed by the peak at $B \approx 0.2$ T, corresponding to the condition $2R_c = d$. This peak is well known for the antidot lattices at $g > 1$ and originates from the so-called pin-ball trajectory surrounding an antidot (the trajectory is numbered by *1* in the inset to Fig. 3a). As is seen from Fig. 3c, the second commensurate peak, corresponding to the condition $2R_c = (\sqrt{2} - 1)d$, is observed at $g \approx 1$. This peak is associated with the trajectory *2* inside the billiard. The positions of the commensurability peaks show that we really deal with the lattice of closely situated antidots with $d \approx a$ and $d \gg d - a$. The Sinai billiards between the antidots have the area $S = d^2(1 - \pi/4)$ and contain a large number of electrons $N \gg 1$. In our case we have $S = 0.5\ \mu m^2$, $N \approx 70$ for $d = 0.7\ \mu m$, and $S = 0.36\ \mu m^2$, $N \approx 50$ for $d = 0.6\ \mu m$. It is important that both the main commensurability peak and NMR are conserved at the transition from $g > 1$ to $g \ll 1$.

The behavior of NMR is shown in Fig. 4 in more detail. It is characterized by two distinguishing features: (i) for all states with $0.05 < g < 2$ NMR is cut off at the same magnitude of the magnetic field $B \approx 0.05$ T; (ii) NMR noticeably increases with decreasing $g$. Figure 4a shows that at $g = 0.05$ it reaches a considerable value about 40%. It should be noted that the higher the resistivity, the stronger the temperature dependence of NMR, and it is even stronger than $g(T)$. For $g > 1$ NMR can be attributed to the effects of weak localization in open chaotic billiards [12], because it has relatively small amplitude and Lorentzian line-shape. The behavior of NMR for $g \ll 1$ is surprising. It increases by an order of magnitude, reaching a considerable value comparable to the total resistance of the sample, while the line-shape of NMR is described by a Lorentz curve of the same width. The width is equal to $\Delta B_1 = 27 \pm 2$ mT for the sample AG219. It corresponds to a half magnetic flux quantum through the area of the billiard that is equal to $d^2(1 - \pi/4)$. The fact that the width is determined by the magnetic flux quantum is well seen from the comparison of NMR for the

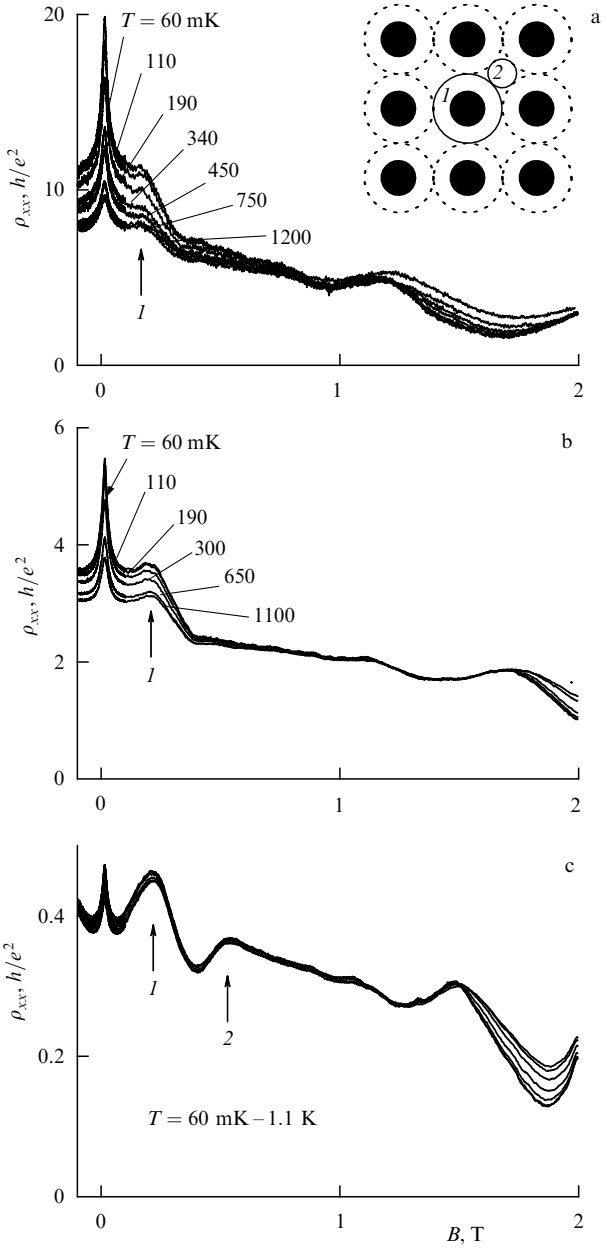


**Figure 3.** Magnetoresistance (MR) traces at different temperatures for different values of the conductivity (sample AG219): $g = 0.05$ (a), $g = 0.18$ (b), $g = 2.2$ (c). The inset to (a) shows a schematic view of antidot lattice (black circles show the etched regions, dashed lines are the boundary of depletion region, *1* — an electron trajectory around antidot, *2* — an electron trajectory between antidots.

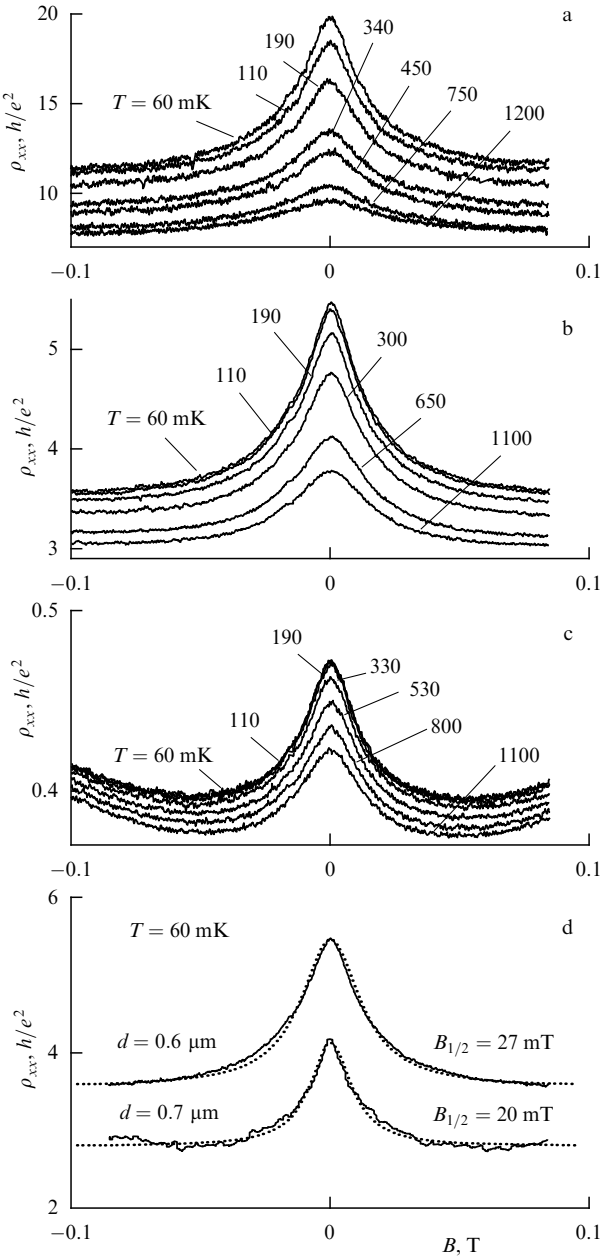


**Figure 4.** NMR curves for the sample AG219 (a,b,c). Experimental and calculated NMR curves for the antidot lattices with two different periods $d = 0.6$ μm (sample AG219) and $d = 0.7$ μm (sample AG35). Solid lines are the experimental curves, dotted lines are the calculated Lorentz ones, $B_{1/2}$ is the width of the Lorentz curves (d).

samples with two different periods 0.6 μm and 0.7 μm. As it is clearly seen from the Fig. 4c the width of NMR curve for the period 0.7 μm equals $\Delta B_2 = 20 \pm 2$ mT, that is $\Delta B_1/\Delta B_2 = 0.7^2/0.6^2$. Thus, at $g \ll 1$ we observe NMR which is very similar to weak localization NMR in chaotic open billiards [2]. In hexagonal lattice the area of the billiards is equal to $d^2(\sqrt{3}/4 - \pi/8)$. It means that the width of NMR curve for the lattice should be approximately 5 times larger than for the same curve in square lattice with the same period. Figure 5 shows the results obtained for hexagonal lattice. It is seen that they support this suggestion. Thus, all NMR experiments strongly indicate that we deal with the chaotic weak localization in open ballistic Sinai billiards.

Let us discuss the results obtained. First turn to the temperature dependence at the transition from $g > 1$ to $g \ll 1$. It differs from the conventional picture of the metal–insulator transition in 2D electron systems. This picture is based on the concept of Anderson localization of electrons, though it were the model of minimal metallic conductivity (MMC) or the scaling theory (ST) [18]. According to this concept, in a macroscopic 2D system, the transition should occur at $k_F l \sim 1$ or $g \sim 1$ from the metallic behavior (as in MMC model) or from the weak localization (as in ST) to the strong localization characterized by the exponential temperature dependence of the activation type (hopping conductivity) or of the Mott type (variable range hopping conductivity). In

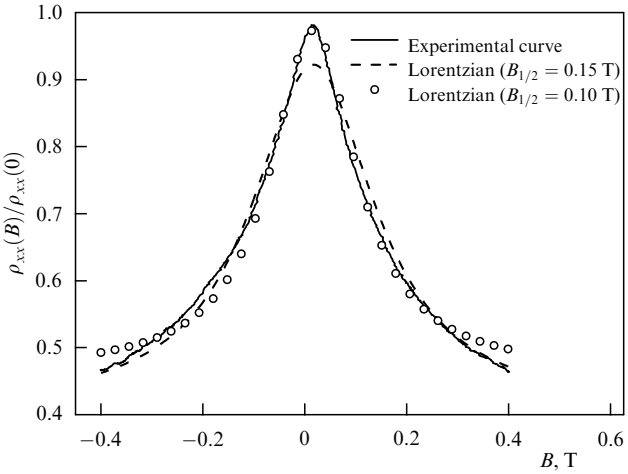


**Figure 5.** Experimental and calculated NMR curves for hexagonal lattice with the period $d = 0.6$ μm ($T = 60$ mK).

real systems the transition can be quite complicated, but for $g \ll 1$ the state with hopping conductivity is always realized [12, 13]. We know only one work [19] in which the linear temperature dependence for $g \ll 1$ was observed in thin $In_2O_3$ films. Recently a similar system has been considered theoretically [20]. Within this model, the metal grains with $g \gg 1$ are coupled by tunneling in such a way that the conductivity of the macroscopic system was low, $g \ll 1$. At $g \ll 1$, owing to inelastic electron–electron scattering, the linear dependence $g(T)$ was obtained in [20] in a wide temperature range. The dependence changes to the exponential one at $T \ll e^2/C$, where $C$ is the capacitance of a metal grain. Our results are not in agreement with the predictions of this theory. Firstly, in our case $g(T)$ is weaker than linear dependence. Secondly, it is observed at $T \ll e^2/C$, because the Coulomb energy for our samples $e^2/2C \approx 15-25$ K. This means that the model of metal lakes coupled by weak tunneling junctions cannot explain the low conductivity of the lattice of the Sinai billiards. The effects of Coulomb blockade are not manifested in the experiment, because one observes no features in $g(V_g)$ dependence. So, we have to assume that at $g \ll 1$ the coupling between the billiards is stronger than that provided by tunneling. The behavior of the lattice in the magnetic field supports this assumption. In Figure 3 one can see the Shubnikov–de Haas oscillations which give the electron density in the lattice saddle points connecting the billiards. It coincides with the density determined from the Hall effect measurements that should give the concentration in these points [21]. The electron density in these points changes weakly with the strong change of $g$. It decreases only by about 30% while $g$ drops by a factor of 30, and its magnitude, equal to $4.1 \times 10^{10}$ cm$^{-2}$, is only three times less than $N_S$ inside the billiard even for the state with the lowest value of $g$. This means that the Fermi level in the saddle point lies several meV above the barrier at $g \ll 1$, and an electron should move ballistically through the 'bottleneck' to go from one billiard to another. The behavior of commensurability peak and of NMR supports this picture. Hence, we come to a paradoxical conclusion that 2D lattice of Sinai billiards coupled via conducting 'bottleneck' can have very low conductivity, $g \ll 1$, but simultaneously exhibits the properties typical of metallic ballistic systems rather than of insulators. This conclusion is in contradiction with the standard picture of metal–insulator transition in 2D systems. It should be noted that percolation supports this fact even stronger because it leads to quasi-one-dimensionality. Let us discuss possible reasons for the situation and consider it from the weak localization side at first. The transition from the weak to strong localization, caused, for example, by the decrease of temperature, should be accompanied by the increase of the phase coherence length. As a consequence, a number of localized trajectories should increase until all the trajectories become localized at $T = 0$. In the systems under study it can be somewhat hampered, since an electron can loose the phase coherence inside a billiard before it leaves for the other billiard through the 'bottleneck'. A simple estimation gives for the dwell-time of the electron inside a billiard $\tau = 10^{-8}$ s. The collimation effects can only increase this time. The estimation shows that $\tau$ can be larger than the time of phase coherence, which is of the order of $\tau_\varphi = 10^{-9}$ s at 40 mK. This means that even at the lowest available temperature an electron can loose the phase coherence on the length scale $L = d$. Then the resistance is the classical sum of the resistances of individual billiards, which can yield any value of $g$. The situation discussed is to some extent similar to that considered in Ref. [20]. In our system, the quantum dots are connected by the conducting 'bottleneck' instead of the tunnel barrier as in Ref. [20]. Obviously, it should lead to the weaker temperature dependence of the conductivity, that is just observed in our experiments. Nevertheless, it is not clear what happens at $T \to 0$, because the Coulomb blockade effects are not observed in our case. The description of the system from the strong localization side is complicated, because one can not start from the ground state of electron in the well, for it represents a multilevel system with the large ($\sim 100$) number of electrons. In any case the description of 2D lattice of coupled Sinai billiards and the phenomena described in the present paper is a challenge to the theory of quantum transport in the condensed matter.

This work was supported by RFBR (Grant 99-02-16756), by NATO Linkage Grant PST.CTG.976830, by CNRS–RFBR Grant PICS628-RFBR98-22008, and by the Russian Ministry of Industry, Science and Technology through the program "Statistical Physics".

## References

1. Marcus C M et al. *Phys. Rev. Lett.* **69** 506 (1992)
2. Chang A M et al. *Phys. Rev. Lett.* **73** 2111 (1994)
3. Chang A M et al. *Phys. Rev. Lett.* **76** 1695 (1996)
4. Folk J A et al. *Phys. Rev. Lett.* **76** 1699 (1996)
5. Taylor R P et al. *Phys. Rev. Lett.* **78** 1952 (1997)
6. Ensslin K, Petroff P M *Phys. Rev. B* **41** 12307 (1990)
7. Weiss D et al. *Phys. Rev. Lett.* **66** 2790 (1991)
8. Gusev G M et al. *Pis'ma Zh. Eksp. Teor. Fiz.* **54** 369 (1991) [*JETP Lett.* **54** 364 (1991)]
9. Lorke A, Kotthaus J P, Ploog K *Phys. Rev. B* **44** 3447 (1991)
10. Baskin E M et al. *Pis'ma Zh. Eksp. Teor. Fiz.* **55** 649 (1992) [*JETP Lett.* **55** 678 (1992)]
11. Budantsev M V et al. *Surf. Sci.* **361/362** 739 (1996)
12. Ando T, Fowler A B, Stern F *Rev. Mod. Phys.* **54** 437 (1982)
13. Jiang H W et al. *Phys. Rev. Lett.* **71** 1439 (1993); Wang T et al. *Phys. Rev. Lett.* **72** 709 (1994); Hughes R J F et al. *J. Phys.: Condens. Mat.* **6** 4763 (1994); Shahar D, Tsui D C, Cunningham J E *Phys. Rev. B* **52** R14372 (1995)
14. Lutjering G et al. *Surf. Sci.* **361/362** 925 (1996)
15. Nihey F, Kastner M A, Nakamura K *Phys. Rev. B* **55** 4085 (1997)
16. Shklovskiĭ B I, Efros A L *Elektronnye Svoĭstva Legirovannykh Poluprovodnikov* (Electronic Properties of Doped Semiconductors) (Moscow: Nauka, 1979) [Translated into English (Berlin: Springer–Verlag, 1984)]

17. Gusev G M et al., in *Proc. of 12th Intern. Conf. High Magnetic Fields in Semiconductors Physics, Würzburg, 1996* (Eds G Landwehr, W Ossau) (Singapore: World Scientific, 1997) p. 391
18. Lee P A, Ramakrishnan T V *Rev. Mod. Phys.* **57** 287 (1985)
19. Ovadyahu Z, Imry Y *J. Phys. C* **18** L19 (1985)
20. Imry Y, Stern A, Sivan U *Europhys. Lett.* **39** 639 (1997)
21. Efros A L *Solid State Commun.* **65** 1281 (1988)

# Chaotic quantum transport in superlattices

T M Fromhold, A A Krokhin, P B Wilkinson, A E Belyaev, C R Tench, S Bujkiewicz, F W Sheard, L Eaves, M Henini

**Abstract. We report a new type of quantum chaotic system in which the classical Hamiltonian originates from the intrinsically quantum mechanical nature of the device. The system is a semiconductor superlattice in a magnetic field. The energy–momentum dispersion curves can be used to calculate semiclassical orbits for electrons confined to a single miniband. When a magnetic field is applied along the superlattice axis ($x$-direction), the electrons perform Bloch oscillations along the axis with cyclotron motion in the orthogonal plane. But when the magnetic field is tilted away from the $x$-direction, the orbits are chaotic, and have a spatial width along the superlattice axis, which is much larger than the amplitude of the Bloch oscillations. This is because the tilted field transfers momentum between the $x$- and $z$-directions, thereby delocalizing the electron path. This type of chaotic dynamics is *fundamentally different* to that identified in our previous studies of double–barrier resonant tunneling diodes. We investigate the relation between the orbits of the effective Hamiltonian, and the quantum states of the superlattice. In the regime of strong chaos, the wave functions have a highly diffuse structure which extends across many periods of the superlattice, just like the corresponding classical orbits. This chaos-induced delocalization increases the current flow through real devices. By contrast, in the stable domain the electron orbits remain localized along the paths of particular quasi-periodic orbits. We use theoretical and experimental current–voltage curves to show how the onset of chaos manifests itself in the transport properties of two- and three-terminal superlattice structures, and identify current oscillations associated with classical resonances. We also consider analogies with ultra-cold atoms in an optical lattice with a tilted harmonic trap.**

We investigate the semiclassical motion of electrons confined to the lowest miniband of a GaAs/(AlGa)As superlattice with a high magnetic field. Tilting the magnetic field away from the superlattice axis induces a transition from stable regular motion to chaotic dynamics which have an intrinsically quantum-mechanical origin associated with the miniband dispersion relation. The onset of chaos delocalizes the semiclassical orbits and corresponding quantized eigenstates. We use a classical kinetic formalism to calculate the electron drift velocity versus applied bias voltage, and find that chaos-induced orbital delocalization can produce a large increase in the electrical conductivity.

Most experimental studies of the quantum properties of systems with chaotic classical dynamics have been performed either on atoms or on low-dimensional semiconductor structures [1]. The first experiments were performed on highly-excited hydrogenic atoms in a magnetic field, and revealed periodic fluctuations in the photo-absorption spectra, associated with unstable periodic electron paths [2, 3]. These orbits modulate the energy level density, and produce 'scarred' wave functions in which the probability density is concentrated along the classical path [4, 5]. More recently, ultra-cold atoms in a phase-modulated optical lattice, formed using two counter-propagating laser beams to set up an electromagnetic standing wave [6], have provided experimental evidence for dynamical localization in a quantum-mechanical 'kicked rotor' [7]. In semiconductor physics, chaotic electron transport has been explored in two-dimensional quantum dots [1, 8, 9], antidot arrays [10], and in resonant tunneling diodes (RTDs) [1, 11–19]. The RTDs contain a square potential well, in which electrons follow chaotic classical paths when a tilted magnetic field is applied [1, 11–19]. In the regime of strong chaos, scarred states in the well generate series of resonant peaks in measured tunneling characteristics [12, 15].

In this paper, we consider how semiconductor superlattices (SLs) with a tilted magnetic field can be used to provide a new type of quantum chaotic system that is accessible to experiment. In contrast to previous structures that have been used to study quantum chaos, the effective classical Hamiltonian for electron motion in the SLs has an intrinsically quantum-mechanical origin associated with the electronic energy bands. For low electric fields, SLs have well-defined minibands. The energy–wavevector dispersion relations define an effective Hamiltonian that determines semiclassical [20] orbits for electrons confined to a single miniband. Our calculations for this system show that tilting an applied magnetic field $\mathbf{B}$ at an angle $\theta$ to the SL axis induces a transition from stable to chaotic classical motion. The onset of chaos delocalizes both the classical orbits and the corresponding quantum wave functions, and thereby increases the electron drift velocity.

The potential energy of an electron in a SL structure is schematically shown in Fig. 1. Here we consider GaAs/(AlGa)As SLs containing barriers of width $b = 1.25$ nm and wells of width $w = 9.5$ nm. The SL period $a = b + w$. The Al fraction is taken to be either 0.3, for which the miniband width $\Delta = 26$ meV, or 1, which gives $\Delta = 8$ meV. We have investigated electron transport in the first miniband of the SL, using a tight-binding approximation for the energy–wavevector dispersion relation

$$E(\mathbf{k}) = \frac{\Delta(1 - \cos k_x a)}{2} + \frac{\hbar^2(k_y^2 + k_z^2)}{2m^*} ,$$

where $m^* = 0.07m_e$ is the electron effective mass for motion in the $(y, z)$ plane. The $E(\mathbf{k})$ relation defines an effective Hamiltonian for electron motion in electric and magnetic fields that are small enough to preserve the miniband structure. This Hamiltonian is obtained from $E(\mathbf{k})$ by adding the electrostatic potential energy due to the electric field $\mathbf{F} = (-F, 0, 0)$ and making the substitution $\hbar\mathbf{k} = \mathbf{p} \rightarrow \mathbf{p} + e\mathbf{A} = m^*\mathbf{v}$, where

**T M Fromhold, A A Krokhin, P B Wilkinson, A E Belyaev, C R Tench, S Bujkiewicz, F W Sheard, L Eaves, M Henini** School of Physics and Astronomy, University of Nottingham, Nottingham NG7 2RD, UK
**A A Krokhin** Universidad Autonoma de Puebla, Puebla, Mexico
**S Bujkiewicz** Institute of Physics, Wroclaw University of Technology, Wybrzeze, Wyspianskiego 27, 50–370, Poland